

Starbursts in barred spiral galaxies

V. Morphological analysis of bars ^{*}

S. Chapelon^{1,2}, T. Contini^{1,3}, and E. Davoust¹

¹ Observatoire Midi-Pyrénées, UMR 5572, 14 Avenue E. Belin, F-31400 Toulouse, France

² Laboratoire d'Astronomie Spatiale du CNRS, B.P. 8, 13376 Marseille Cedex 12, France

³ European Southern Observatory, Karl-Schwarzschild-Str. 2, D-85748 Garching bei München, Germany

Received ??; accepted ??

Abstract. We have measured the bar lengths and widths of 125 barred galaxies observed with CCDs. The dependence of bar strength (identified with bar axis ratio) on morphological type, nuclear activity, central and mid-bar surface brightness is investigated.

The properties of the bars are best explained if the sample is divided into early- (< SBbc) and late-type galaxies, and into active (starburst, Seyfert or LINER) and normal galaxies. We find that galaxies with very long bars are mostly active and that normal late-type galaxies have a distinct behavior from the three other groups of galaxies. We confirm earlier findings that active late-type galaxies tend to have both stronger and longer bars than normal ones. An important result of this paper is that early-type galaxies do not share this behavior : they all tend to have strong bars, whether they are active or not. We also find correlations between bar strength and relative surface brightness in the middle and at the edge of the bar, which are not followed by normal late-type galaxies.

These results are interpreted in the light of recent numerical simulations and paradigms about galaxy evolution. They suggest that normal late-type galaxies represent the first stage of galaxy evolution, and that bars in early- and late-type galaxies do not have the same properties because they have a different origin.

Key words: Galaxies: photometry – Galaxies: starburst
– Galaxies: structure

Send offprint requests to: Davoust, davoust@obs-mip.fr

^{*} Based on observations obtained at the 2 meter telescope of Observatoire du Pic du Midi, operated by INSU (CNRS)

1. Introduction

The presence of a bar strongly modifies the internal dynamics of spiral galaxies, as evidenced by the deviations from circular motion in the velocity maps of barred galaxies; the isoveLOCITY curves in the bar tend to align with the bar major axis. Numerical simulations have shown that these non-circular motions induced by the presence of a bar are toward the center of the galaxy. Inside corotation, the dissipative gaseous component loses angular momentum to the stars and falls inward (e.g. Schwarz 1984, Wada & Habe 1992, Friedli & Benz 1993), as a result of the torque exerted by the bar.

The rate of gaseous inflow depends essentially on the bar strength, which is the ratio of the force of the bar to that of the axisymmetric disk. The bar strength in turn depends on the bar axis ratio and on its mass. The rate of inflow also depends on the bulge-to-disk mass ratio, but not on the bar pattern speed nor on the gas mass (Friedli & Benz 1993).

This bar driven fueling provides an obvious mechanism for producing the activity that is often observed in the center of barred spiral galaxies (e.g. Contini et al. 1998). However, the role of the bar on starburst (Hawarden et al. 1996) or Seyfert activity (Ho et al. 1997) in spiral galaxies remains controversial.

In view of these conflicting results, a detailed study of the correlation between bar strength and starburst activity would be welcome. A first step in this direction is the morphological study of Martin (1995), who measured the bar axis ratio of 136 barred galaxies on prints of blue photographs displayed in the atlas of Sandage & Bedke (1988). He found an apparent correlation between bar axis ratio and star formation activity. Martinet & Friedli (1997) selected 32 late-type galaxies from Martin's sample and showed that the galaxies with the strongest star formation activity had both thin and long bars, but that this was not a sufficient condition for violent star formation.

The present paper is a further step in the study of the relation between bar strength and starbursts. It is based on a morphological study of bars, and uses the bar axis ratio as an estimate of the bar strength, as in Martin (1995) and in Martinet & Friedli (1997). But several significant improvements are made. Our investigation rests on CCD images, which lend themselves to more quantitative measurements than photographic prints, and provide the photometric properties of the bars. The choice of a red filter for the observations reduces the perturbing effect of dust. We implement a method for measuring the axis ratio which is not influenced by the perturbing presence of the bulge.

Our main goal is to check whether the results of Martin (1995) and of Martinet & Friedli (1997) still hold using our CCD data and method of measurement. Since our sample of galaxies is very different, biased toward starbursting and early-type galaxies, we can also hope to discriminate universal properties from those which are merely caused by selection effects. Finally, we take advantage of the large database accumulated on our sample (Contini 1996, Contini et al. 1997) to look for correlations between bar morphology and other galaxian properties, such as starburst age, oxygen abundance, and neutral hydrogen mass.

2. The samples of barred galaxies

We used two samples of barred galaxies for this study. The first one is composed of all the Markarian galaxies that are barred and have been detected by IRAS. It contains 144 galaxies, for many of which we obtained CCD images, low-resolution CCD spectra, neutral hydrogen and CO profiles (Contini 1996).

CCD images of 121 galaxies of this sample were obtained during several runs at the Bernard Lyot 2-meter telescope of Observatoire du Pic du Midi, with a 1000×1000 Thomson CCD (pixel size $0.24''$ on the sky). The seeing was good, with a median value of about $1.5''$. During one of those runs, we also observed NGC 6764 for one of the papers in this series (Contini et al. 1997). The details of the observations can be found in Contini (1996).

From this sample, we selected the 100 galaxies which have a measurable bar. We decided to make the measurements on the images taken in the red (R' Cousins; for a definition, see de Vaucouleurs & Longo 1988) band, because dust lanes which perturb the measurements are less conspicuous in that band than in the bluer ones. The calibration of the zero point of the magnitude scale was done by indirect procedures. The photometric constants of 34 galaxy images were obtained using published aperture photometry (de Vaucouleurs & Longo 1988); the accuracy of the zero point is 0.1 mag. For the 66 other galaxies, we had to rely on a mean photometric constant for the night, with a resulting accuracy of only 0.4 mag.

We also needed a comparison sample, with no bar or no starburst. Since we did not have images of ordi-

nary Markarian starburst galaxies, we took the second option and selected our comparison sample among the 113 galaxies observed by Frei et al. (1996), whose calibrated CCD images are publicly available by ftp at astro.princeton.edu/frei/Galaxies. We selected the galaxies of that sample that were classified barred in LEDA. After eliminating galaxies with no measurable bar (because of misclassification or high inclination), we were left with 26 galaxies. We made the measurements on the images taken in the red (Cousins or Gunn) band, as for the first sample. The zero point calibration of these images is very good, with an average uncertainty of about 0.05 mag (if NGC 4498 is excluded, which has an uncertainty of 0.4 mag.).

Table 1 gathers all the information on these galaxies necessary for our analysis. The galaxy name is in col. 1; the numerical morphological type and inclination (from LEDA) in col. 2 and 3; the distance (in Mpc, estimated from the redshift given in LEDA and a Hubble constant of $75 \text{ km s}^{-1} \text{ Mpc}^{-1}$) in col. 4; the absolute magnitude (from LEDA) in col. 5; the HI mass and FIR and $H\alpha$ luminosities (in log of solar masses, solar luminosities and $\text{erg cm}^{-2}\text{s}^{-1}$ respectively, from Contini 1996) in col. 6, 7 and 8; the central (nearly central for Seyferts) oxygen abundance (from Contini et al. 1998; from the literature for the comparison sample) in col. 9; the IRAS flux ratio S_{25}/S_{100} (in log, computed from the fluxes given in Bica et al. 1995, or the Faint Source Catalogue) followed by L (when an upper limit) in col. 10; the spectral classification (from Contini et al. 1998; from the literature for the comparison sample) in col. 11. No IRAS flux ratio is given when the fluxes at 25 and $100\mu\text{m}$ are both upper limits. Table 1 is given in electronic form only.

Table 1. Physical parameters of the sample galaxies. This Table is available in electronic form only

Early-type galaxies are defined as earlier than SBbc ($t < 4$), and late-types as SBbc and later. The IRAS flux ratio is used to distinguish between starburst/Seyfert and more quiescent galaxies. The former, which we hereafter call 'active', have a ratio $\log(S_{25}/S_{100}) \geq -1.2$; the others are called 'normal'. It is true that we have independently determined the spectral type of the Mrk galaxies by optical spectroscopy (Contini et al. 1998), but we have not done so for the sample of Frei et al. (1996), and we need a uniform criterion for both samples. The adopted criterion also has the advantage of being the same as that used by Martinet & Friedli (1997), and thus allows a comparison of our results with theirs. This criterion is essentially a measure of the star formation efficiency. Coziol et al. (1998) have in fact shown that IRAS colors are very efficient for separating starburst, quiescent and Seyfert galaxies.

3. Method of measurement of the bar parameters

The method adopted by Martin (1995) for measuring the length and width of bars is visual and relies on photographic prints in the blue band. He estimates that, with this method, the uncertainty is about 20%. He defines the semi-major axis of the bar as the length from the galaxy center to the sharp outer tip where spiral arms begin, and the semi-minor axis as the length from the center to the edge of the bar, oval, lens or spheroidal component, measured perpendicularly to the major axis.

Our CCD images allow us in principle to make a sophisticated numerical analysis, including adjustment of ellipses to the bar. However, such a method is fraught with pitfalls which have been outlined by Wozniak et al (1995), and we preferred to rely on a simpler method. We first extract a 3-pixel wide photometric profile along the major axis of the bar. The semi-major axis a of the bar is the distance from the center of the galaxy to where the bar obviously ends. This is where the surface brightness profile abruptly changes slope to become steeper; this also coincides with the origin of the spiral arms. This measurement is not automatic, it relies on the subjective judgement of where the bar ends, and is comparable to that of Martin (1995). It is hopefully more reliable, since our CCD images have a large dynamic range and were taken in the red band.

On the other hand, the method for measuring the width of the bar departs significantly from that of Martin (1995). We believe that his method overestimates the bar width, because it includes the effect of the bulge. To measure the width, we extract two photometric profiles (also three pixels wide) along the minor axis of the bar at two symmetrical distances of $a/2$ from the center and take their average. The semi-minor axis b of the bar is the distance from the bar major axis to the same isophotal level as where the tip of the bar was measured. This method is comparable to that of Friedli & Benz (1993).

4. Results of the bar measurements

The results of our bar measurements on CCD images are summarized in Table 2. The galaxy name is in col. 1; the position angle of its major axis (from LEDA; from our images if not in LEDA) in col. 2; the angle Φ between the bar and galaxy major axes (from our images) in col. 3; the measured semi-major and semi-minor axes (in arcsec) in col. 4 and 5; the deprojected semi-major and semi-minor axes (in arcsec) in col. 6 and 7; the deprojected axis ratio in col. 8; the ratio of deprojected major axis to corrected blue diameter at the isophote 25 ($2a/D_c$, hereafter normalized bar length, where D_c is from LEDA) in col. 9; the surface brightness along the bar at the center (μ_c), where the semi-minor axis is measured (at half the distance to the end of the bar, μ_m) and at the tip of the bar (μ_b), in mag.arcsec⁻² in col. 10, 11 and 12. Table 2 is given in

electronic form only. To give the reader a feeling for what the different types of bars look like, we show examples of each category in Fig. 1.

Table 2. Bar characteristics of the sample galaxies. This Table is available in electronic form only

The bar measurements were deprojected using the equations given by Martin (1995). NGC 6764, Mrk 1326 and Mrk 1452 were observed in V only. For NGC 6764, the bar surface brightnesses were transformed to R' using the mean $(V - R')$ color of the galaxy computed from de Vaucouleurs & Longo (1988). For Mrk 1326 and 1452, the bar surface brightnesses were transformed to R' using the mean $(V - R')_e$ for their respective morphological type (Buta & Williams 1995).

The fact that we chose to normalize the bar length by D_c deserves an explanation. Martin (1995) and Martinet & Friedli (1997) used D_{25} , probably because they thought that absorption affects the galaxy diameter and bar length in the same way. Our images, however, are in the red band-pass, and, in all logic, we should use a red isophotal diameter. We did measure the isophotal diameter D_{24R} corresponding to a surface brightness of 24 mag.arcsec⁻² on our images, and compared it to D_{25} . For the Frei sample, there is a good correlation with a small scatter, from which we derived the mean relation $D_{25} = 1.04 \times D_{24R} - 0.03 \times t$. For the Mrk sample, on the other hand, the scatter is much larger, because two thirds of the images suffer from poor photometric calibration. We thus had to resort to D_c . From the above relation, we estimate that the error induced by this choice (compared to a reliable D_{24R}) is not larger than 5%, and reduced by the fact that we distinguish early- and late-type galaxies in the analysis.

The repeatability of our measurements was involuntarily verified when we later discovered that NGC 4123, one of Frei et al.'s (1996) galaxies, is also Mrk 1466. The comparison between the two sets of measurements for this galaxy gives an estimate of the external errors. The relative uncertainty on the bar axis ratio is 20%, while that on the bar length is less than 5%. Since this galaxy is not in de Vaucouleurs & Longo (1988), the errors on the estimated surface brightnesses reach 0.5 mag. Only the measurements performed on our image of NGC 4123 were used in the subsequent analysis.

We have compared our measurements with those of Kormendy (1979) for 13 galaxies in common and those of Martin (1995) for 15 galaxies in common. We agree qualitatively with them, except for NGC 4487, where Martin (1995) finds a bar length and width half the size of ours; we checked that there was no scale error between the two images of that galaxy. We find average differences $(a_{us} - a_K) = -2.6''$ and $(a_{us} - a_M) = 2.8''$. In other words, our estimates for the semi-major axis are intermediate between

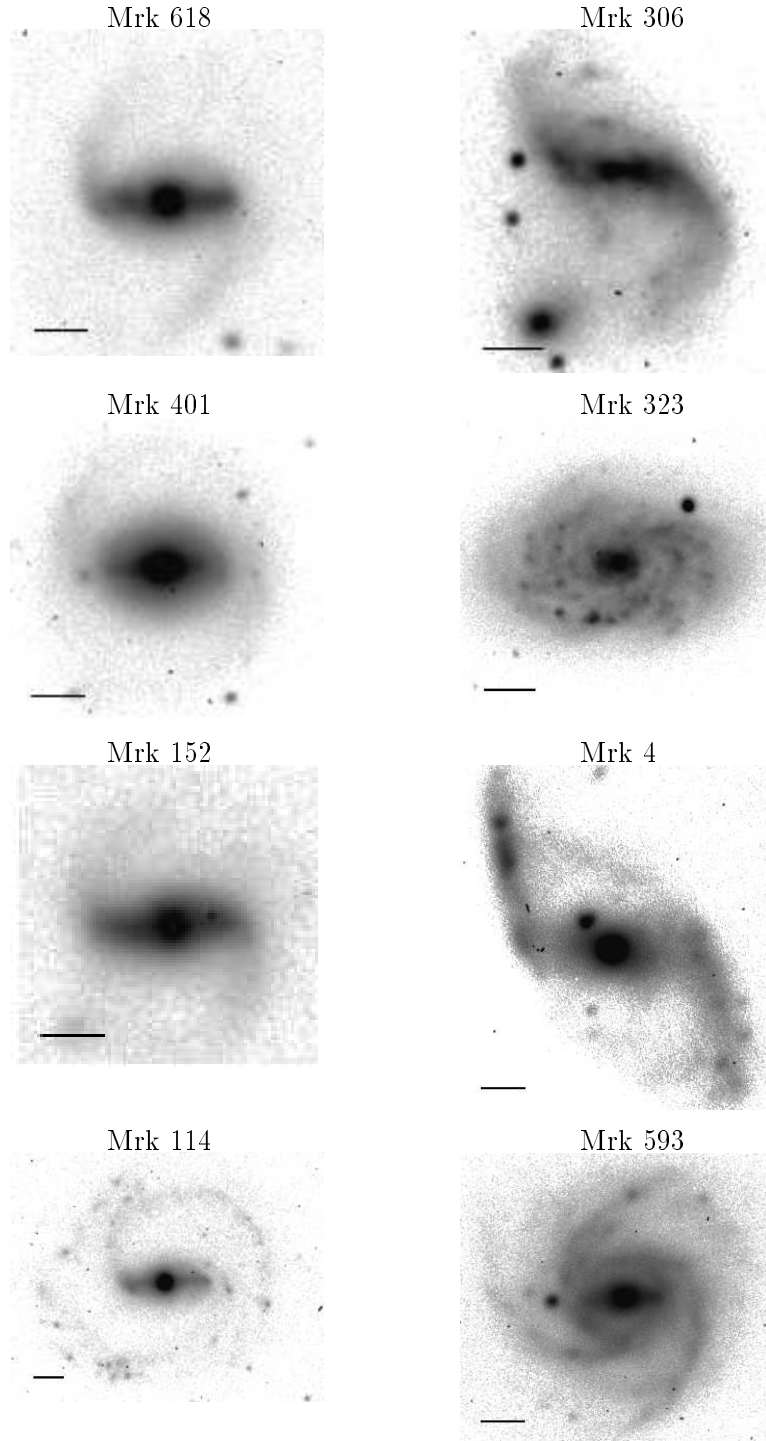


Fig. 1. Examples of each category of bars. Early-type galaxies are on the left and late-type ones on the right. From top to bottom : strong, weak, long and short bars. All images have been flipped and rotated in such a way that the bar is horizontal and the spiral pattern is winding counterclockwise. The scale is indicated by a 10-arcsec long horizontal line

those of Martin and Kormendy. These are marginally significant results because it is not obvious to decide exactly where the bar ends. Martin finds larger semi-minor axes than us by $2.0''$ on the average, because he measures them from the center of the galaxy. For that reason, he also finds thicker bars than us by 0.14 on the average.

The largest discrepancies with Martin (1995) are on the angle between the bar and galaxy major axes, which in turn produce large differences in the axis ratios corrected for inclination, $(b/a)_i$.

We consider that $(b/a)_i$ is a good measure of the bar strength, and subsequently use the terms strong and weak rather than thin and thick. Strong bars are defined as having $(b/a)_i < 0.5$; this is consistent with Martin (1995) who puts the limit at 0.6, but has weaker bars than us by 0.14 on the average.

5. Correlations with other galaxian properties

There are 125 different galaxies in the total sample, but in the astrophysical analysis of the data, we eliminated 23 galaxies for which the IRAS flux ratio $\log(S_{25}/S_{100})$ is either an upper limit (and much larger than -1.2) or unknown altogether. In the analyses involving the deprojected bar axis ratio $(b/a)_i$, we also eliminated another 13 galaxies for which the deprojected bar axis ratio differed by more than 0.2 from the apparent one, because the uncertainties in the deprojection factor and in the true geometry of the bar mainly affect the deprojected semi-minor axis, and thus the deprojected bar axis ratio.

5.1. Bar characteristics and morphological type

The mean value of the deprojected bar axis ratio for the total sample (125 galaxies) is $(b/a)_i = 0.31 \pm 0.12$. For the sample restricted to reliable axis ratios and IRAS color (89 galaxies), it is 0.30. The 57 early-type galaxies seem to have a slightly stronger bar (0.28 ± 0.10) than the 32 late-type ones (0.34 ± 0.14), but the difference is not statistically significant.

The galaxies of our sample have on the average rather strong bars; less than 5% of them are in fact weak, compared to 36% in Martin's (1995) sample (using the appropriate limit for each sample). The 121 galaxies of his sample with a measured bar axis ratio have a mean ratio of 0.55 ± 0.19 (or about 0.45 if we correct for the difference in method of measurement). These differences in bar strength may be partly due to the fact that we have more early-type galaxies (60% vs 18%) and more active galaxies (57% vs 36%) than Martin (1995). The two samples are thus quite different.

There is marginal evidence that early-type galaxies have longer bars than late-type ones, relative to the galaxy size. Such a difference is expected on dynamical grounds (Elmegreen & Elmegreen 1985). The values of the normalized bar length $2a/D_c$ for the two types are 0.37 ± 0.17

Table 3. Mean values of the bar strength $(b/a)_i$ and normalized length $2a/D_c$ for the different groups of galaxies of our sample. N is the number of galaxies in the group

Group	N	$(b/a)_i$	N	$2a/D_c$
$t \geq 4$, normal	19	0.37 ± 0.18	23	0.22 ± 0.08
$t \geq 4$, active	13	0.29 ± 0.08	14	0.35 ± 0.12
$t < 4$, normal	19	0.29 ± 0.11	22	0.32 ± 0.14
$t < 4$, active	38	0.27 ± 0.11	43	0.36 ± 0.14

and 0.28 ± 0.12 respectively. This confirms earlier findings by Elmegreen & Elmegreen (1985) and Martin (1995). We have computed the mean bar lengths $2a/D_{25}$ of early- and late-type galaxies in Martin's sample, and find 0.33 and 0.17 respectively. The late-type galaxies of Martin have much shorter bars than ours, but, since his galaxies are mostly normal, they should be compared to our normal late-type galaxies, which have a mean bar length of 0.23, thus quite near his value.

5.2. Bar characteristics and starburst activity

The properties of the bars in relation to starburst activity are only revealed once the sample is broken into two groups, early- and late-type galaxies.

Our results are summarized in Table 3, which gives the mean values of the bar strength and length for the different groups of galaxies. The numbers N of galaxies in the different groups are not the same for the statistics on bar strength and length, because galaxies with large inclination correction were excluded from the analysis and statistics involving bar strength. Our results are also shown in Figs. 2 and 3, where the relation between bar strength and length for the two types of galaxies is plotted. They reveal two main properties of bars with respect to activity:

- The normal late-type galaxies (empty squares in Fig. 2) stand out from the three other groups in that there are no very long bars ($2a/D_c > 0.4$). For this group, there is a good correlation between bar length and strength, of equation : $2a/D_c = -0.50(b/a)_i + 0.43$, with a correlation coefficient of 0.85.

- Galaxies with very long bars ($2a/D_c > 0.4$) are also strong and mostly active, while galaxies with short bars ($2a/D_c < 0.2$) are mostly normal.

On the other hand, no trend of bar strength with activity appears, probably because our sample is biased toward strong bars.

In Figs. 2 and 3, we distinguish Seyferts and LINERs (triangles) from starburst galaxies (squares). In fact, the two Figures show that the Seyferts and LINERs are undistinguishable from starbursts as far as bar characteristics are concerned. The only remarkable difference between the two types of active galaxies is that most of those with

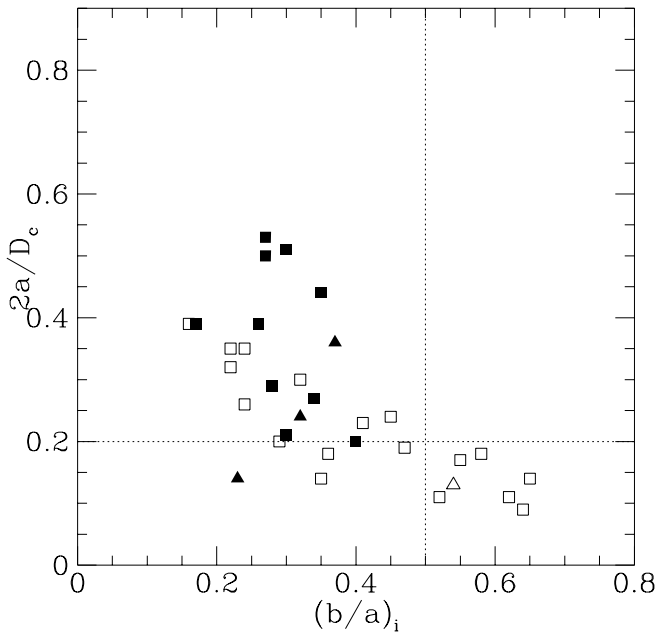


Fig. 2. Relation between bar strength and length in late-type ($t \geq 4$) galaxies. Filled symbols indicate galaxies with $\log(S_{25}/S_{100}) \geq -1.20$ and open symbols galaxies with $\log(S_{25}/S_{100}) < -1.20$. Seyferts and LINERs are indicated by triangles, other galaxies by squares. The limits between strong and weak bars and between long and short bars are indicated by dotted lines

$\log(S_{25}/S_{100}) > -0.9$ are Seyferts or LINERs. It turns out that, with the adopted activity criterion, a small minority of Seyferts and LINERs falls in the category of normal galaxies.

We now turn to a comparison with results from the literature. Using 32 late-type galaxies from the sample of Martin (1995), Martinet & Friedli (1997) showed that all the late-type galaxies with large star formation rates have both strong and long bars, but that some more quiescent galaxies also do share these properties. We confirm this result, using the 32 late-type galaxies with reliable $(b/a)_i$ of our sample, 5 of which are in common with Martinet & Friedli's sample, but with independent measurements (see Fig. 2). On the other hand, this is not true for the 57 early-type galaxies of our sample (see Fig. 3). Most of them, whether they are active or not, have strong and long bars, just like the active late-type galaxies.

Our Fig. 2 should be compared to Fig. 3 of Martinet & Friedli (1997). These authors chose a value of 0.18 for the limit between long and short bars; we adopted a value of 0.2 for comparison, since our bar estimates are slightly larger than those of Martin (1995) for galaxies in common. Our Figs. 2, 3 and 6 suggest that a value of 0.4 would in fact be a more realistic limit for general purposes.

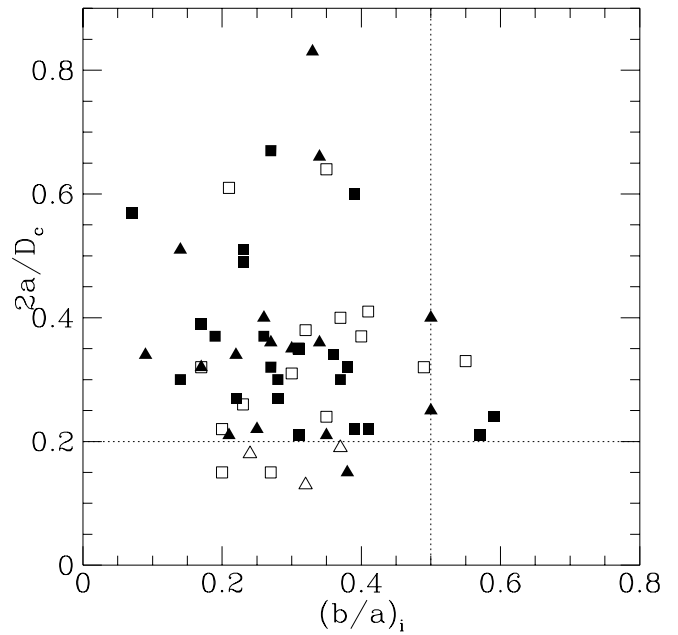


Fig. 3. Same as Fig. 2 for early-type ($t < 4$) galaxies

The cumulative distribution of bar axis ratios shows that all the active late-type galaxies of our sample and 63 (± 5)% of the normal ones have strong bars. Martin (1995) finds that about 71% of his active galaxies and 59% of the quiescent ones have a strong bar; our active galaxies thus have much stronger bars than Martin's, but the strength of the quiescent ones are comparable.

5.3. Photometric properties of the bars

We have measured the surface brightness along the bar at the center and at the distances $a/2$ and a from the center. Hereafter we call these quantities μ_c , μ_m and μ_b respectively; we also determined $\Delta\mu_c = \mu_m - \mu_c$ and $\Delta\mu_b = \mu_b - \mu_m$. The reason for computing two surface brightness differences rather than one is that the influence of the bulge is (hopefully) confined to the first one only. While μ_c depends on seeing, it is still a good indicator of the nuclear surface brightness. We again break the sample into early- and late-type galaxies for comparing the photometric and morphological properties of the bars. The three main results are:

- The normal late-type galaxies again stand out from the three other groups. They have a fainter central surface brightness (μ_c) and a smaller $\Delta\mu_c$. This is partly due to the fact that normal late-type galaxies have fainter μ_c and shorter bars than the other groups. The main result to keep in mind here is that the middle of the bar is about two magnitudes fainter than the nucleus, or about one magnitude fainter in the case of normal late-type galaxies.

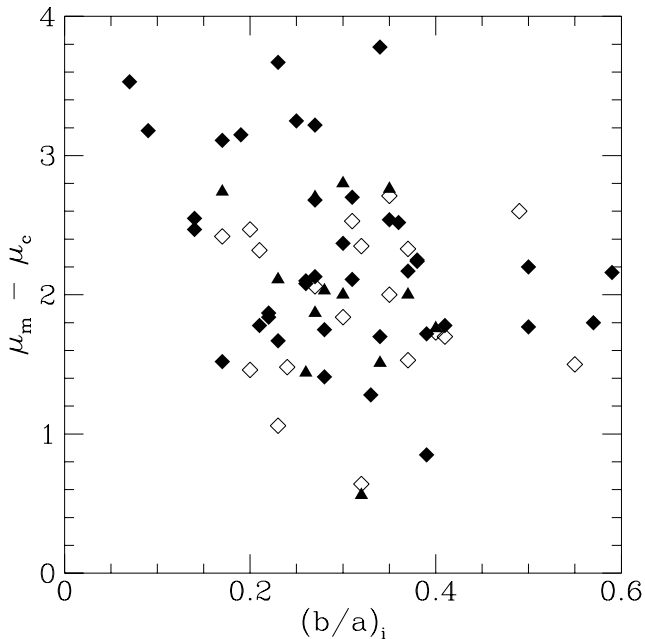


Fig. 4. Bar strength as a function of surface brightness difference between center and mid-bar, for early- ($t < 4$; diamonds) and late-type (triangles) galaxies; open symbols indicate normal galaxies and filled ones active galaxies. The normal late-type galaxies have not been plotted because they do not share the correlation

– The surface brightness difference between middle and end of the bar ($\Delta\mu_b$) is independent of morphological type or activity and is of about 0.44 mag. One can also note that $\Delta\mu_b$ is smaller than $\Delta\mu_c$ and that $\Delta\mu_c$ depends on morphological type for normal galaxies only (it is larger for early types); these last two results are due to the influence of the bulge which is more important in early-type galaxies.

– There is a correlation between bar strength and $\Delta\mu_b$, and an opposite one between bar strength and $\Delta\mu_c$, which are again shared by all groups except the normal late-types (see Figs. 4 and 5). Stronger bars have a larger $\Delta\mu_c$ and a smaller $\Delta\mu_b$, and vice versa. In other words, weak bars tend to have a flatter overall surface brightness gradient than strong ones.

The photometric properties of bars have already been studied in the past. Elmegreen & Elmegreen (1985) and Elmegreen et al. (1996) find that bars in early-type galaxies tend to have flat¹ light profiles and those in late-type galaxies tend to have exponential profiles outside the bulge region. Comparisons with our results are difficult because the nature of these surface brightness gradients is determined by comparison with the gradient in the disk, and the bar strength is not determined. Nevertheless, using bar strength determined by Martin (1995) for the 4 late-

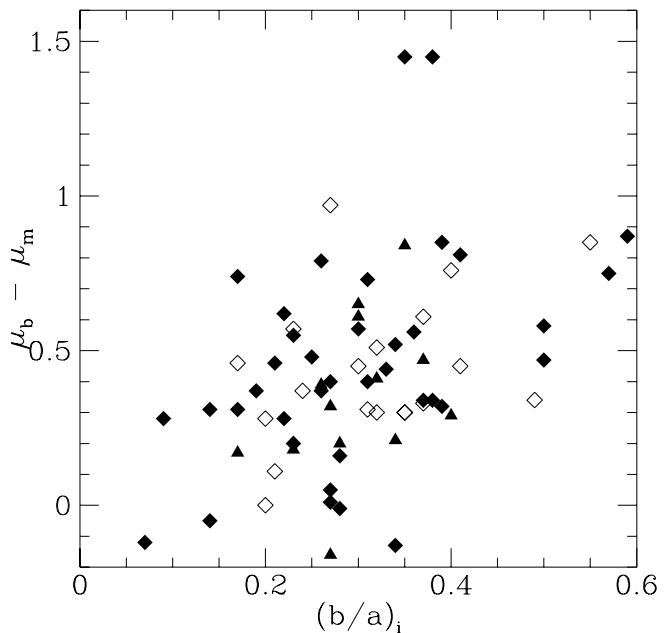


Fig. 5. Same as Fig. 4 for the surface brightness difference between middle and end of bar.

type galaxies with exponential profiles (NGC 3359, which has a very strong bar, is considered to have a flat profile in their second paper), we find a mean value of 0.42, thus rather weak, which is expected for bars with steep outer brightness profiles. Ohta et al. (1990) have determined the surface brightness profiles of 6 early-type galaxies. They find rather flat outer gradients, less than 0.5 mag, for 4 out of 6 galaxies; all of them have strong bars.

5.4. Bar strength and central oxygen abundance

We have investigated a possible dependence of bar characteristics on the oxygen abundance measured in the center of the galaxies. The relation between bar length and central oxygen abundance (in solar units) for early- and late-type galaxies is displayed in Fig. 6. While there seems to be no trend with bar strength, we find that there are no galaxies with high oxygen abundance ($O/H > 1.4$) and very long ($2a/D_c > 0.4$) bars.

We have also studied the relation between bar length and strength and the oxygen abundance gradient along the bar. The results are described in paper IV of this series (Considère et al., in preparation).

A search for correlations between bar characteristics and blue, far infrared and $H\alpha$ luminosities and neutral hydrogen mass did not reveal any meaningful trends, even when normalizing these quantities by the blue luminosity.

¹ Note that flat does not mean constant but straight

Table 4. Mean values of the nuclear surface brightness (μ_c) and of the surface brightness differences between center and mid-bar ($\Delta\mu_c$) and between middle and end of bar ($\Delta\mu_b$) for the different groups of galaxies of our sample. N is the number of galaxies in the group

Group	N	μ_c	$\Delta\mu_c$	$\Delta\mu_b$
$t \geq 4$, nor	23	18.68 ± 0.83	0.95 ± 0.41	0.37 ± 0.20
$t \geq 4$, act	14	17.86 ± 0.94	2.00 ± 0.62	0.42 ± 0.34
$t < 4$, nor	22	17.96 ± 0.63	1.94 ± 0.53	0.48 ± 0.25
$t < 4$, act	43	17.85 ± 0.89	2.25 ± 0.70	0.46 ± 0.34

6. The role of bars in the evolution of galaxies

We now use the bar properties determined in the previous section to discuss the possible role of bars in shaping the evolution of galaxies.

The first point is to understand why normal late-type galaxies stand out from the three other groups. This can be seen in two ways, depending on whether the activity or the morphology of the galaxy is considered the determining factor. In the first case, the normal early-type galaxies stand out because they behave like active galaxies; in the second case, the active late-type galaxies should be singled out, because they have the same properties as the early-type galaxies. In either case one reaches the conclusion that early- and late-type galaxies differ in their bar properties, and thus presumably in the way the bar originates and the galaxy evolves.

This concurs with the results of numerical simulations by Noguchi (1996), who concludes that the bars of late-type galaxies slowly form as a result of bar instability in the disk, whereas the bars of early-type galaxies form more rapidly (within one disk rotation period) in tidal interactions. He also finds that tidally induced bars have flatter surface density profiles than spontaneous bars. Even though he does not study the dependence of this profile on bar strength, there are indications in his paper that induced bars are stronger than spontaneous bars, which is expected if interactions induce a stronger perturbation than natural disk instabilities. This would confirm the relation that we find between strength of the bar and flatness of the outer surface brightness profile.

Now, to explain the specificity of normal late-type galaxies, one has to consider the overall evolution of galaxies. According to the latest paradigm (Pfenniger 1998), galaxies evolve from late to early type by forming a bar which dissolves into a bulge, then grows again to form a more massive bulge. In this scenario, a normal late-type galaxy, which initially develops a short bar, becomes active as the bar gets stronger and longer and funnels more gas toward the center to feed star formation. In the later evolution, a new and initially strong bar arises in the wake

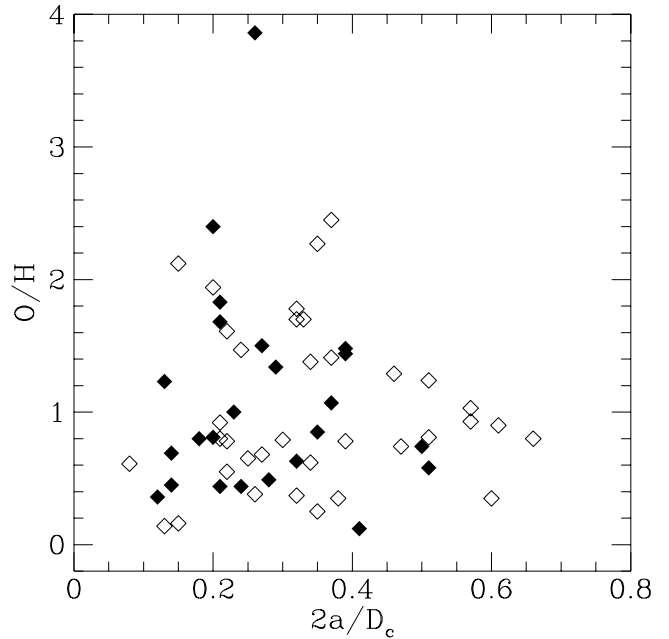


Fig. 6. Normalized bar length as a function of central oxygen abundance (in solar units) for early- (open diamonds) and late-type (filled diamonds) galaxies. There are no galaxies with long bars and high oxygen abundance

of a tidal perturbation, grows longer and star formation resumes after sufficient gas has been accreted. The evolution thus proceeds, alternating between barred and unbarred structure, until there is no more gas to be funnelled toward the center.

The correlation between bar strength and $\Delta\mu_c$ is readily understood in this context: a stronger bar favors central star formation, which in turn enhances the brightness contrast between the bar and the nucleus. The fact that stronger bars have flatter outer profiles, predicted by the simulations, is probably best understood in terms of stellar dynamics. In strong bars, the stellar orbits are more elongated and the stars spend more time near apogalacticon, thus enhancing the surface brightness of the outer regions of the bar. However, this explanation rests on the assumption that these are regular orbits; chaotic orbits are likely to fill larger regions and to smooth out the density contrast (Wozniak & Pfenniger 1999).

Finally, the absence of very long bars with high oxygen abundances can be explained in two different ways. The first one, which was suggested to us by Daniel Friedli, is that long bars allow gas from regions further out, where the oxygen abundances are very low, to reach the central regions and thus to dilute the central abundances. Alternatively, star formation increases the amount of dust, which can hide the extremities of the bars. We have indeed noticed that the bars of our galaxies are longer in K than in the R band (Bergougnan et al., in preparation); a

similar trend has also been noticed by Friedli et al. (1996). We are indebted to Hervé Wozniak for pointing this out to us. The correct explanation might be a combination of these two possibilities.

Acknowledgements. Data from the literature were obtained with the Lyon Meudon Extragalactic database (LEDA), supplied by the LEDA team at CRAL-Observatoire de Lyon (France). We thank the staff of Observatoire du Pic du Midi for assistance at the telescope. We also thank Christophe Bordry and David Teyssier for their contribution to the statistical analysis of the data, as well as Alessandro Boselli, Daniel Friedli, Hervé Wozniak and Ron Buta for helpful comments on this paper.

References

- Bicay M.D., Kojoian G., Seal J., et al., 1995, ApJ 98, 369
 Buta R., Williams K.L., 1995, AJ 109, 543
 Contini T., 1996, Ph. D. thesis, Université Paul Sabatier, Toulouse, France
 Contini T., Considère S., Davoust E., 1998, A&AS 130, 285 (paper III)
 Contini T., Davoust E., Considère S., 1995, A&A 303, 440 (paper I)
 Contini T., Wozniak H., Considère S., Davoust E., 1997, A&A, 324, 41 (paper II)
 Coziol R., Contini T., Davoust E., Considère S., 1997, ApJ, 481, L67
 Coziol R., Torres C.A.O, Quast G.R., Contini T., Davoust E., 1998, ApJS, 119, 239
 Elmegreen B.G., Elmegreen D.M., 1985, ApJ 288, 438
 Elmegreen B.G., Elmegreen D.M., Chromey F.R., et al., 1996, AJ 111, 2233
 Frei Z., Guhathakurta P., Gunn J., Tyson J.A., 1996, AJ 111, 174
 Friedli D., Benz W., 1993 A&A 268, 65
 Friedli D., Wozniak H., Rieke M., et al., 1996, A&AS 118, 461
 Hawarden T.G., Huang J.H., Gu Q.S., 1996, in : Barred Galaxies, Buta R., Crocker D.A., Elmegreen B.G. (eds.), Proc. IAU Coll. 157, ASP Conference Series, p. 54
 Ho L.C., Filippenko A.V., Sargent W.L.W., 1997, ApJ 487, 591
 Kormendy, J., 1979, ApJ 277, 714
 de Vaucouleurs A., Longo G., 1988, The University of Texas Monographs in Astronomy No. 5
 Martin P., 1995, AJ 109, 2428
 Martinet L., Friedli D., 1997, A&A, 323, 363
 Noguchi M., 1996, ApJ 469, 605
 Ohta K., Hamabe M., Wakamatsu K.I., 1990, ApJ 357, 71
 Pfenniger D., 1998, in : Abundance profiles: diagnostics tools for galaxy history, Friedli D., Edmunds M.G., Robert C., Drissen L. (eds.), ASP Conference Series, p. 237
 Sandage A., Bedke J., 1988, Atlas of galaxies useful for measuring the cosmological distance scale (NASA, Washington DC)
 Schwarz, M.P., 1984, MNRAS 209, 93
 Wada K., Habe A., 1992, MNRAS 258, 82
 Wozniak H., Friedli D., Martinet L., Martin P., Bratschi P., 1995, A&AS 111, 115

Wozniak H., Pfenniger, D., 1999, in: "Impact of Modern Dynamics in Astronomy", Proc IAU Coll. 172, J. Henrard & S. Ferraz-Mello (eds), Celestial Mechanics, in press

Table 1: Physical characteristics of the sample galaxies

Name (1)	Type (2)	Incl. (3)	Dist. (4)	M_{abs} (5)	M(HI) (6)	L(FIR) (7)	L(H α) (8)	O/H (9)	$\log(S_{25}/S_{100})$ (10)	Sp.t (11)
Mrk 1	3.1	55.1	66.2	-19.77	9.57	10.13			-0.53	Sy2
Mrk 2	0.6	31.7	75.8	-21.00	9.47	10.64		1.61	-0.91	STB
Mrk 4	6.0	62.4	73.4	-20.02	9.57	10.37	40.30		-1.19	STB
Mrk 10	3.1	70.2	119.4	-22.96	10.63	10.34		0.65	-0.95	Sy1
Mrk 12	5.0	38.0	55.9	-21.24	9.97	10.37		0.80	-1.38	STB
Mrk 13	3.1	32.5	21.7	-17.84	9.55	8.59	39.54	0.61		STB
Mrk 21	3.6	49.2	115.1	-20.96		10.11	39.59	1.03	-1.08	STB
Mrk 42	2.7	38.0	98.5	-20.01		9.80	40.40	0.93		Sy1
Mrk 52	-0.7	61.6	28.5	-19.40	8.99	9.70	40.84	0.78	-0.73	STB
Mrk 79	3.0	3.8	90.8	-21.65	9.89	10.24			-0.49	Sy2
Mrk 87	1.0	45.3	51.0	-20.22	9.86	9.79	40.14		-1.49	STB
Mrk 90	3.8	29.6	59.4	-20.06	9.17	9.74	40.64		-1.14	STB
Mrk 109	8.0	49.9	123.4	-20.14	10.15	10.20	0.42		-0.80L	STB
Mrk 114	3.1	35.8	103.1	-21.29	10.30	10.41	40.94		-1.28	STB
Mrk 122	2.0	66.4	90.4	-21.25		10.20	40.25		-1.40	STB
Mrk 152	2.7	67.4	94.3	-20.77		9.94	40.70		-0.73	LIN
Mrk 161	4.3	52.3	82.1	-21.19	9.99	10.49	41.07	0.74	-1.05	STB
Mrk 179	5.3	39.7	47.4	-20.07	9.34	9.59	39.37	1.44	-1.15	STB
Mrk 185	6.0	42.6	43.9	-20.80	9.95	9.91	39.64		-1.50	STB
Mrk 188	5.3	39.5	35.0	-20.48	9.69	10.00	40.45	3.86	-1.41	STB
Mrk 213	1.1	49.2	44.7	-20.61	9.40	10.07	40.74	0.37	-0.99	STB
Mrk 271	3.1	43.9	103.9	-21.89		10.49	41.15	0.14	-1.37	Sy2
Mrk 281	3.1	36.3	32.5	-20.85	9.74	9.99			-1.30	STB
Mrk 291	1.0	49.1	143.6	-20.57		10.16				Sy1
Mrk 300	-0.1	59.6	157.5	-21.20	9.85	10.43	42.14	0.74		STB
Mrk 306	4.3	52.3	76.5	-20.69	9.86	9.87	40.39	0.63	-1.14L	STB
Mrk 307	4.6	37.2	75.9	-21.33	9.82	10.26		1.00	-1.35	STB
Mrk 319	1.0	55.8	109.7	-21.63	9.98	10.99			-1.12	STB
Mrk 323	6.0	43.8	59.5	-20.64	9.49	10.30	40.31		-1.36	STB
Mrk 326	4.0	49.8	49.2	-20.19	9.75	10.13		1.83	-0.92	STB
Mrk 332	4.7	24.8	33.6	-20.03	9.06	9.95	40.17	0.81	-1.18	STB
Mrk 339	4.0	6.3	71.5	-20.01	9.73	9.75			-0.96	LIN
Mrk 353	3.4	58.5	63.6	-20.35	9.33	10.36	41.59	0.55	-1.00	STB
Mrk 358	4.0	42.7	182.5	-21.84	10.17	10.44				Sy1
Mrk 359	3.4	36.2	68.8	-20.46	8.85	9.92			-0.60	Sy1
Mrk 373	4.0	44.5	81.2	-19.73	9.27	10.23	41.58	0.58	-0.93	STB
Mrk 382	4.6	30.0	136.7	-21.09	9.77	9.96				Sy1
Mrk 384	3.0	50.6	63.2	-20.79	9.29	10.37	40.06		-1.07	STB
Mrk 386	3.8	66.8	48.3	-20.96	9.90	9.51			-1.03L	STB
Mrk 401	0.5	27.4	23.7	-18.31	8.82	9.30	39.12	1.47	-0.85	STB
Mrk 446	3.1	40.6	96.6	-21.42	9.91	10.31	40.52	0.80	-0.95	STB
Mrk 474	0.0	49.8	154.4	-20.73		10.33			-0.73L	Sy1
Mrk 479	4.0	60.6	82.6	-21.18	10.04	10.27	41.28	0.45	-1.36	STB
Mrk 493	3.0	14.3	128.6	-20.97	9.82	10.23			-0.83	Sy1
Mrk 533	3.8	24.5	117.5	-21.81	10.35	11.04			-0.63	Sy2
Mrk 538	3.1	41.7	37.8	-20.38	9.81	10.30			-0.61	LIN
Mrk 545	1.1	49.1	62.6	-21.67	9.90	10.73	41.65	0.92	-1.15	STB
Mrk 571	3.4	48.6	68.6	-20.78	9.80	10.04	41.33		-1.07L	STB
Mrk 575	1.0	39.2	73.7	-20.92	9.69	10.40	40.41		-1.04	STB
Mrk 592	3.0	37.2	100.9	-21.27	9.92	10.35			-0.93	STB
Mrk 593	5.3	6.6	110.5	-21.05	10.22	10.31	40.54		-0.79L	STB
Mrk 602	4.0	36.8	37.6	-19.52	9.71	9.87	41.38	1.34	-0.95	STB

(1)	(2)	(3)	(4)	(5)	(6)	(7)	(8)	(9)	(10)	(11)
Mrk 617	4.9	35.1	62.3	-20.93	9.53	11.20	42.18	0.69	-0.65	LIN
Mrk 618	3.0	42.8	137.9	-22.18	9.89	10.87		0.81	-0.73	Sy1
Mrk 620	1.0	44.3	27.2	-20.23	9.29	9.83	41.09	0.16	-0.87	Sy2
Mrk 665	-1.4	32.1	107.4	-21.07	9.58	10.16	41.35	0.68	-1.06	STB
Mrk 686	1.3	47.6	58.9	-20.72	9.18	9.63		0.12	-1.14	Sy2
Mrk 691	5.3	53.4	45.9	-21.02	9.93	10.12	41.14	1.50	-1.16	STB
Mrk 703	2.1	2.1	50.7	-20.74	10.01	10.19			-1.09	STB
Mrk 710	2.5	51.0	19.8	-18.71	9.12	9.18	40.09	1.24	-1.00	STB
Mrk 712	3.6	62.8	61.6	-20.64	9.75	9.70	40.78	0.35	-0.95	STB
Mrk 731	-1.3	49.0	19.0	-18.55	8.14	9.19	39.25	1.94	-0.78L	STB
Mrk 752	4.1	35.3	81.5	-20.83	9.85	9.90	40.67	0.44	-0.80L	STB
Mrk 759	5.2	37.7	29.7	-20.13	9.61	9.79	40.33		-1.21	STB
Mrk 781	4.6	31.5	38.3	-20.11	9.50	9.66	39.94	0.49	-0.96L	STB
Mrk 799	3.0	51.4	42.8	-20.91	9.59	10.48		2.27	-1.08	STB
Mrk 814	3.2	70.6	54.3	-20.43	9.80	9.83	40.03	0.38	-1.25	STB
Mrk 861	4.9	21.3	60.5	-19.87	9.20	9.84			-0.94	STB
Mrk 871	4.9	60.3	136.8	-21.74	9.87	10.30			-0.49	Sy1
Mrk 874	3.6	59.5	58.8	-19.79	9.33	9.35	40.35	0.35	-1.16	STB
Mrk 896	2.7	56.0	103.2	-21.70		10.05			-0.91	Sy1
Mrk 898	3.1	52.3	70.1	-20.08	9.16	9.79		1.78	-0.75L	STB
Mrk 917	1.0	21.6	100.0	-20.98	9.38	10.74			-0.99	Sy2
Mrk 955	4.2	57.3	139.2	-21.47	9.64	10.49			-0.64L	Sy2
Mrk 968	3.7	23.3	59.3	-20.52	9.84	9.66			-0.77L	STB
Mrk 1009	3.1	54.7	57.1	-21.15	9.89	9.82	40.35	0.78	-1.29	STB
Mrk 1050	1.0	54.2	67.3	-20.61	9.59	10.52	41.68		-1.03	STB
Mrk 1058	4.8	64.1	70.2	-19.94		9.74	41.51	0.12	-0.91	Sy2
Mrk 1066	-1.1	54.7	50.0	-20.23		10.54	41.97	0.25	-0.73	Sy2
Mrk 1067	1.6	41.0	57.7	-20.53	9.67	10.07	40.42		-1.43	STB
Mrk 1073	3.0	21.5	95.3	-21.56	9.53	11.02	41.49	0.62	-0.90	Sy2
Mrk 1076	3.9	64.3	95.8	-20.48		9.85	41.45	1.29		STB
Mrk 1086	2.7	27.8	118.9	-21.21	9.92	10.25	40.05	0.79	-0.98	STB
Mrk 1088	0.1	20.7	60.6	-21.82	9.43	10.53	41.82	1.38	-1.11	STB
Mrk 1149	0.0	59.9	83.5	-19.85	9.58	9.96				STB
Mrk 1157	-0.1	38.5	62.7	-20.32	9.38	10.06			-0.89	Sy2
Mrk 1180	0.0	43.7	62.1	-21.04		9.90			-1.59L	STB
Mrk 1194	-2.0	52.7	59.0	-21.30	9.47	10.56	41.80		-1.21	STB
Mrk 1200	2.7	7.9	103.6	-20.96	9.77	10.38	40.65		-1.03	LIN
Mrk 1231	0.5	52.6	149.6	-21.14		10.60	40.04		-1.00	STB
Mrk 1273	0.0	57.9	108.0	-20.46		10.11	40.13		-0.91L	STB
Mrk 1291	3.9	36.8	48.1	-20.84	10.08	9.89			-1.31	Sy2
Mrk 1302	3.0	52.3	74.5	-20.35	9.77	9.68		0.90	-0.52L	STB
Mrk 1326	5.9	27.2	18.9	-18.58	8.73	8.83	38.82	1.68	-0.67L	STB
Mrk 1341	5.9	47.7	15.7	-18.91	9.03	9.04	39.02	0.85	-1.30	STB
Mrk 1433	4.1	39.2	256.4	-22.59		10.95	41.35		-1.30	STB
Mrk 1452	4.9	39.0	92.4	-19.90	9.70	9.90	39.31	1.07		STB
Mrk 1466	5.1	42.0	17.7	-19.85	9.65	9.45	40.41	1.48	-0.93	STB
Mrk 1485	3.6	38.5	33.4	-20.82	9.90	9.74	39.71	2.12	-1.43	STB
NGC 2541	6.0	64.7	9.5	-18.77	9.48	9.18		0.36	-0.61L	
NGC 2715	5.2	74.1	21.0	-21.03	9.91	9.33			-1.80	
NGC 3319	6.0	57.6	11.9	-19.52	9.46	8.46		0.44		
NGC 3351	3.1	55.9	10.6	-20.30	9.21	9.49		2.45	-0.91	STB
NGC 3368	1.8	51.1	12.2	-20.96	9.41	9.42		1.41	-1.72	
NGC 3486	5.2	46.0	10.4	-19.63	9.56	9.01			-1.68	
NGC 3726	5.2	48.2	14.2	-20.49	9.78	9.20			-1.34	
NGC 3953	4.0	61.7	16.8	-21.20	9.33	9.83			-1.40	

(1)	(2)	(3)	(4)	(5)	(6)	(7)	(8)	(9)	(10)	(11)
NGC 4088	4.2	72.0	12.8	-20.43	9.64	9.73			-1.36	
NGC 4123	5.1	42.0	17.7	-19.85	9.65	9.45	40.41	1.48	-0.93	STB
NGC 4136	5.2	22.4	9.7	-18.42	9.04	8.41			-1.26L	
NGC 4178	7.2	72.0	5.5	-19.70	9.02	8.46			-1.57L	
NGC 4189	5.9	47.3	28.8	-20.40	9.51	9.69			-1.35	
NGC 4303	4.0	25.4	21.1	-21.88	10.10	10.28		1.23	-1.66	LIN
NGC 4394	2.9	18.9	13.3	-19.28	8.47	8.63			-1.44	
NGC 4487	6.0	46.6	13.2	-19.50	9.17	8.85			-1.18L	
NGC 4498	6.3	59.4	21.0	-19.60	9.11	9.03			-1.35L	
NGC 4548	3.1	36.8	7.3	-20.99	8.17	8.31			-1.74L	
NGC 4579	2.8	38.4	20.9	-21.67	8.99	9.65			-1.53	Sy1
NGC 4593	3.0	47.1	32.8	-21.29	9.33	9.69			-0.82	Sy1
NGC 4654	5.9	53.7	14.6	-20.46	9.46	9.71		2.40	-1.35	
NGC 4725	2.4	48.9	17.7	-21.77	9.94	9.53		1.70	-2.02	
NGC 4731	5.9	69.4	19.5	-20.55	10.03	9.22			-1.56L	
NGC 5377	1.0	60.0	26.8	-20.38	9.23	9.14			-1.32L	
NGC 5850	3.1	36.5	34.8	-21.62	9.76	9.42			-1.54L	
NGC 6384	3.9	51.0	23.6	-21.72	10.10	9.53		1.70	-1.84	
NGC 6764	3.6	58.1	35.7	-21.14	9.67	10.10		0.80	-0.95	LIN

Table 2: Bar characteristics of the sample galaxies

Name (1)	p.a. (2)	Φ (3)	a (4)	b (5)	a_i (6)	b_i (7)	$(b/a)_i$ (8)	$2a/D_c$ (9)	μ_c (10)	μ_m (11)	μ_b (12)
MK 1	86	-10.0	7.14	2.45	7.37	4.24	0.57	0.31	18.57	19.75	19.99
MK 2	170	-135.3	4.65	1.82	5.07	1.99	0.39	0.22	18.54	19.39	19.71
MK 4	12	40.1	19.20	4.68	30.48	8.29	0.27	0.53	18.99	21.69	22.01
MK 10	130	-8.6	13.03	3.94	14.11	11.49	0.81	0.25	17.59	20.40	20.69
MK 12	10	102.8	5.20	3.72	6.53	3.77	0.58	0.18	18.68	19.43	19.87
MK 13	145	-10.0	2.69	0.73	2.70	0.87	0.32	0.08	18.62	19.25	19.67
MK 21	91	3.2	16.45	0.80	16.48	1.23	0.07	0.57	18.41	21.94	21.82
MK 42	31	119.3	8.35	1.80	10.11	1.93	0.19	0.57	18.68	21.24	21.52
MK 52	82	18.0	22.50	6.12	25.92	12.38	0.48	0.39	17.69	20.69	21.08
MK 79	132	-83.6	14.12	3.88	14.14	3.88	0.27	0.36	17.65	20.87	21.27
MK 87	70	-26.6	22.36	6.38	24.54	8.61	0.35	0.64	18.90	20.90	21.20
MK 90	15	162.3	7.17	1.80	7.27	2.05	0.28	0.30	18.44	19.85	20.01
MK 109	36	-6.3	4.46	2.25	4.50	3.48	0.77	0.42	19.12	19.95	20.33
MK 114	155	-16.2	11.53	3.34	11.76	4.06	0.35	0.24	17.73	20.44	20.74
MK 122	165	-44.5	8.47	3.46	16.02	6.62	0.41	0.41	18.13	19.83	20.28
MK 152	17	133.3	9.40	3.20	18.96	6.17	0.33	0.83	19.51	20.79	21.23
MK 161	43	47.0	8.74	2.42	12.03	3.23	0.27	0.50	17.91	19.78	19.62
MK 179	145	-103.0	12.55	4.10	16.15	4.17	0.26	0.39	19.31	20.75	21.14
MK 185	160	-131.4	20.30	5.10	24.66	5.97	0.24	0.35	18.87	20.88	21.27
MK 188	120	9.4	14.95	2.85	15.09	3.67	0.24	0.26	18.00	19.43	20.09
MK 213	130	-2.1	16.59	2.90	16.61	4.42	0.27	0.32	17.31	19.99	20.00
MK 271	117	-24.6	3.30	0.85	3.56	1.13	0.32	0.13	19.00	19.64	19.94
MK 281	85	22.1	49.90	8.80	51.77	10.64	0.21	0.61	18.37	20.69	20.80
MK 291	42	-15.4	6.40	1.90	6.70	2.84	0.42	0.67	18.22	20.56	21.12
MK 300	163	3.0	10.15	2.75	10.19	5.42	0.53	0.47	16.99	19.35	20.10
MK 306	39	135.0	8.55	1.85	11.58	2.50	0.22	0.32	19.02	19.52	19.65
MK 307	60	107.5	6.29	3.10	7.77	3.18	0.41	0.23	18.51	19.59	19.92
MK 319	75	62.7	8.80	2.05	14.50	2.48	0.17	0.39	17.94	19.46	20.20
MK 323	30	-6.0	3.35	1.50	3.37	2.08	0.62	0.11	17.53	18.04	18.33
MK 326	35	81.6	7.20	3.32	11.10	3.37	0.30	0.21	17.70	19.70	20.31
MK 332	55	27.4	8.38	3.17	8.56	3.42	0.40	0.20	17.33	19.09	19.38
MK 339	53	114.0	6.66	2.13	6.70	2.13	0.32	0.24	19.14	19.70	20.11
MK 353	29	-5.0	5.75	1.25	5.82	2.38	0.41	0.22	17.38	19.16	19.97
MK 358	88	52.2	6.20	2.33	7.67	2.67	0.35	0.26	18.66	20.12	20.56
MK 359	10	90.3	5.34	0.60	6.62	0.60	0.09	0.34	15.94	19.12	19.40
MK 373	12	12.9	10.85	2.40	11.11	3.32	0.30	0.51	18.18	20.56	21.21
MK 382	118	59.5	6.15	1.40	6.87	1.46	0.21	0.29	16.87	19.61	20.15
MK 384	113	-40.6	9.28	2.46	11.84	3.34	0.28	0.27	17.74	19.49	19.48
MK 386	167	6.7	12.60	4.62	13.05	11.70	0.90	0.22	17.20	19.30	20.11
MK 401	162	6.7	8.53	4.45	8.54	5.00	0.59	0.24	16.99	19.15	20.02
MK 446	160	9.7	8.96	2.11	9.05	2.77	0.31	0.21	17.03	19.73	20.46
MK 474	153	-2.1	5.00	1.90	5.00	2.94	0.59	0.37	18.27	19.83	20.55
MK 479	5	3.5	4.60	0.80	4.62	1.63	0.35	0.14	17.54	18.62	19.50
MK 493	41	7.8	11.25	1.90	11.26	1.96	0.17	0.32	18.00	21.11	21.42
MK 533	150	-49.2	7.00	2.48	7.40	2.59	0.35	0.21	17.76	20.30	21.75
MK 538	4	134.4	10.80	2.70	12.80	3.18	0.25	0.22	16.75	20.00	20.48
MK 545	8	145.3	11.34	5.61	13.56	7.73	0.57	0.21	19.79	21.59	22.34
MK 571	45	39.2	14.20	2.25	17.46	3.00	0.17	0.32	16.91	19.33	19.79
MK 575	119	-86.3	9.77	2.90	12.61	2.90	0.23	0.49	18.16	19.83	20.03
MK 592	10	156.4	11.15	3.66	11.65	4.46	0.38	0.32	18.82	21.07	22.52
MK 593	37	128.3	8.16	3.02	8.20	3.03	0.37	0.21	19.02	20.05	20.43
MK 602	90	-57.0	10.21	3.15	12.05	3.40	0.28	0.29	17.77	19.80	20.00

(1)	(2)	(3)	(4)	(5)	(6)	(7)	(8)	(9)	(10)	(11)	(12)
MK 617	85	-48.0	5.10	1.19	5.75	1.31	0.23	0.14	16.77	18.88	19.06
MK 618	85	-82.5	10.40	2.00	14.12	2.02	0.14	0.51	18.02	20.49	20.80
MK 620	50	57.6	12.59	5.52	16.31	6.22	0.38	0.15	16.97	19.21	19.55
MK 665	97	73.5	6.58	1.67	7.68	1.69	0.22	0.27	17.11	18.98	19.60
MK 686	150	-18.8	11.40	4.20	12.09	6.04	0.50	0.25	17.77	19.54	20.12
MK 691	45	34.9	11.55	3.30	14.58	4.92	0.34	0.27	16.65	18.16	18.37
MK 703	153	-22.2	20.48	2.77	20.48	2.77	0.14	0.30	17.40	19.95	19.90
MK 710	25	9.8	33.77	4.96	34.51	7.79	0.23	0.51	17.47	20.68	21.23
MK 712	22	4.6	12.45	3.06	12.60	6.67	0.53	0.38	19.16	20.35	21.02
MK 731	10	150.0	12.46	2.96	14.38	4.18	0.29	0.20	18.59	19.46	20.18
MK 752	64	-46.9	6.12	2.63	6.88	2.92	0.42	0.24	19.27	20.33	21.16
MK 759	115	-86.0	6.40	4.21	8.08	4.21	0.52	0.11	17.97	18.80	19.49
MK 781	70	-65.1	16.50	4.53	18.88	4.68	0.25	0.28	18.24	20.43	20.68
MK 799	8	141.0	18.53	5.28	23.59	7.37	0.31	0.35	17.54	19.65	20.05
MK 814	163	-130.5	6.20	1.60	14.75	3.36	0.23	0.26	17.90	18.96	19.53
MK 861	95	-0.2	7.90	2.60	7.90	2.79	0.35	0.44	16.94	19.70	20.54
MK 871	107	18.5	6.35	1.40	7.27	2.71	0.37	0.36	17.86	19.43	19.90
MK 874	154	-20.6	8.90	2.15	10.37	4.04	0.39	0.60	19.23	20.95	21.80
MK 896	38	79.9	7.19	3.76	12.71	3.88	0.31	0.36	18.04	19.90	20.40
MK 898	152	-2.1	10.40	2.10	10.41	3.43	0.33	0.32	17.57	19.14	20.25
MK 917	87	73.0	6.10	1.35	6.52	1.36	0.21	0.21	17.43	19.21	19.67
MK 955	102	15.3	10.52	3.45	11.37	6.22	0.55	0.50	18.82	20.98	23.12
MK 968	55	103.8	9.71	2.61	10.54	2.62	0.25	0.30	17.88	19.90	20.18
MK 1009	145	-7.3	16.50	1.90	16.76	3.27	0.20	0.22	17.72	20.19	20.19
MK 1050	43	6.0	13.85	1.55	13.99	2.64	0.19	0.37	17.49	20.64	21.01
MK 1058	117	-2.4	9.71	3.44	9.75	7.87	0.81	0.41	18.86	20.62	21.85
MK 1066	90	51.1	14.57	4.82	21.64	6.44	0.30	0.35	17.91	20.28	20.85
MK 1067	145	0.5	7.30	1.48	7.30	1.96	0.27	0.15	17.26	19.32	20.29
MK 1073	82	-14.4	11.55	2.40	11.61	2.57	0.22	0.34	16.08	17.92	18.20
MK 1076	13	136.4	6.40	1.32	11.19	2.38	0.21	0.46	19.18	20.50	21.25
MK 1086	3	11.9	8.53	2.82	8.57	3.17	0.37	0.30	18.34	20.51	20.85
MK 1088	85	-66.6	17.97	6.68	19.02	6.75	0.36	0.34	17.47	19.99	20.55
MK 1149	19	144.0	8.82	3.97	12.57	6.83	0.54	0.48	19.92	20.85	21.72
MK 1157	5	83.4	14.07	4.59	17.95	4.61	0.26	0.40	18.08	20.18	20.55
MK 1180	30	20.8	15.11	6.55	15.95	8.78	0.55	0.33	18.27	19.77	20.62
MK 1194	120	-13.9	19.78	4.01	20.74	6.50	0.31	0.35	18.02	20.55	20.86
MK 1200	34	98.7	10.46	3.60	10.56	3.60	0.34	0.36	18.82	20.52	21.04
MK 1231	18	-2.1	11.40	1.85	11.41	3.04	0.27	0.67	19.12	21.25	21.30
MK 1273	97	-49.7	11.60	2.45	18.25	3.52	0.19	1.03	18.94	21.27	21.52
MK 1291	115	1.6	15.70	3.00	15.71	3.75	0.24	0.18	19.32	20.80	21.17
MK 1302	41	1.1	16.55	2.30	16.55	3.76	0.23	0.61	18.87	21.75	21.73
MK 1326	84	90.5	9.75	4.00	10.96	4.00	0.36	0.21	18.33	19.05	19.66
MK 1341	25	99.7	16.38	5.20	24.14	5.29	0.22	0.35	19.14	19.77	20.26
MK 1433	140	13.4	4.75	2.10	4.83	2.67	0.55	0.17	18.59	19.82	20.25
MK 1452	6	134.9	7.55	2.55	8.71	2.94	0.34	0.37	17.02	18.86	20.03
MK 1466	135	-35.2	45.80	7.15	51.62	8.88	0.17	0.39	16.57	19.31	19.48
MK 1485	40	93.3	11.75	3.05	15.01	3.06	0.20	0.15	18.30	19.76	20.04
NGC 2541	165	10.0	22.36	6.30	23.84	14.57	0.61	0.12	20.41	20.93	21.45
NGC 2715	22	0.8	30.20	14.13	30.23	51.42	1.70	0.20	19.17	19.81	19.88
NGC 3319	37	5.1	40.02	8.32	40.42	15.50	0.38	0.21	20.33	20.98	22.05
NGC 3351	13	105.3	48.03	19.99	83.64	21.45	0.26	0.37	17.10	19.18	19.97
NGC 3368	5	108.8	58.20	32.93	89.69	35.45	0.40	0.37	17.20	18.93	19.69
NGC 3486	80	-7.4	17.67	7.24	19.07	12.17	0.64	0.09	17.82	18.89	19.15
NGC 3726	10	21.0	35.12	7.58	37.82	10.96	0.29	0.20	18.54	19.99	20.13
NGC 3953	13	40.1	24.59	7.89	38.38	13.71	0.36	0.18	17.33	18.75	19.20

(1)	(2)	(3)	(4)	(5)	(6)	(7)	(8)	(9)	(10)	(11)	(12)
NGC 3953	13	40.1	24.59	7.89	38.38	13.71	0.36	0.18	17.33	18.75	19.20
NGC 4088	43	9.3	36.10	8.00	40.35	25.53	0.63	0.24	18.54	19.38	19.54
NGC 4123	134	-31.0	42.97	10.64	47.37	13.44	0.28	0.36	18.51	20.39	20.48
NGC 4136	62	-44.0	13.51	5.86	17.53	11.42	0.65	0.14	19.20	20.15	20.36
NGC 4178	30	0.7	44.84	6.46	44.88	20.90	0.47	0.30	19.98	20.61	21.07
NGC 4189	85	29.4	16.05	5.92	18.19	8.14	0.45	0.24	19.19	20.28	20.66
NGC 4303	162	24.0	16.96	8.64	26.48	14.17	0.54	0.13	17.29	18.76	19.13
NGC 4394	103	42.0	32.53	6.79	40.30	12.89	0.32	0.38	17.60	19.95	20.46
NGC 4487	100	-5.9	23.09	7.50	23.23	10.89	0.47	0.19	19.62	20.31	20.84
NGC 4498	133	-14.7	25.09	4.54	27.31	8.71	0.32	0.30	19.85	20.52	20.80
NGC 4548	150	-84.2	40.59	15.04	50.60	15.08	0.30	0.31	18.25	20.09	20.54
NGC 4579	95	-39.8	31.79	11.30	35.65	13.23	0.37	0.19	17.41	18.94	19.55
NGC 4593	55	0.0	44.13	15.02	44.13	22.07	0.50	0.40	18.83	21.03	21.50
NGC 4654	128	-10.2	30.00	13.74	30.86	22.96	0.74	0.20	19.47	20.05	20.30
NGC 4725	35	6.8	102.61	33.33	103.53	50.46	0.49	0.32	18.52	20.47	20.81
NGC 4731	85	45.0	35.34	5.54	75.20	11.78	0.16	0.39	19.87	20.20	20.44
NGC 5377	20	20.6	46.07	16.09	53.95	30.64	0.57	0.50	18.03	20.18	20.70
NGC 5850	140	-23.4	54.38	17.32	56.69	20.93	0.37	0.40	17.76	20.09	20.42
NGC 6384	30	5.0	30.49	15.97	65.88	62.59	0.95	0.33	17.34	19.08	19.97
NGC 6764	62	12.6	43.73	5.71	48.74	16.72	0.34	0.66	15.96	19.74	19.61